One-sentence summary: Contrary to previous reports, wild-type p53 can interact with p73 to promote cell stress–induced apoptosis.

Editor's summary:
Another look at p53-p73 interactions
The transcription factor p53 critically regulates cell survival or death in response to cellular stress. Mutations in p53 are common in cancer and alter its interactions with other proteins and, consequently, with cell fate–specific genes. Mutant p53 binds to and inhibits its family member p73, thereby promoting cell survival instead of cell death in response to cell stress. It was believed that this interaction with p73 was specific to mutant p53. However, Wolf *et al*. found that wild-type p53 can bind p73 to promote stress-induced cell death. Phosphorylation of wild-type p53 by the cell stress–responsive kinase JNK caused a conformational change that mirrored the regional structure of the mutant and enabled its binding to p73 but, unlike mutant p53, the wild-type protein could still bind to apoptotic gene targets. These findings refine our understanding of p53 interactions and specifically p53-p73 coordination in the cell stress response.

Mutant and wild-type p53 form complexes with p73 upon phosphorylation by the kinase JNK

Eric R. Wolf[1†], Ciaran P. M[c]Atarsney[2†], Kristin E. Bredhold[2], Amber M. Kline[2], and Lindsey D. Mayo[12*]

[1]Department of Biochemistry and Molecular Biology, Indiana University School of Medicine, Indianapolis, Indiana, 46202.

[2]Herman B Wells Center for Pediatric Research, Indiana University School of Medicine, Indianapolis, Indiana, 46202.

†These authors contributed equally to this manuscript.

*Corresponding author. Email: ldmayo@iu.edu.

Abstract

The transcription factors p53 and p73 are critical to the induction of apoptotic cell death, particularly in response to cell stress that activates c-Jun N-terminal kinase (JNK). Mutations in the DNA-binding domain of p53, which are commonly seen in cancers, result in conformational changes that enable p53 to interact with and inhibit p73, thereby suppressing apoptosis. In contrast, wild-type p53 reportedly does not interact with p73. Here, we found that JNK-mediated phosphorylation of Thr^{81} in the proline-rich domain (PRD) of p53 enabled wild-type p53, as well as mutant p53, to form a complex with p73.

This is the author's manuscript of the article published in final edited form as:
Wolf, E. R., McAtarsney, C. P., Bredhold, K. E., Kline, A. M., & Mayo, L. D. (2018). Mutant and wild-type p53 form complexes with p73 upon phosphorylation by the kinase JNK. Sci. Signal., 11(524), eaao4170. https://doi.org/10.1126/scisignal.aao4170

Structural algorithms predicted that phosphorylation of Thr^{81} exposes the DNA-binding domain in p53 to enable its binding to p73. The dimerization of wild-type p53 with p73 facilitated the expression of apoptotic target genes [such as those encoding p53-upregulated modulator of apoptosis (PUMA) and Bcl-2-associated X protein (BAX)] and, subsequently, the induction of apoptosis in response to JNK activation by cell stress in various cells. Thus, JNK phosphorylation of mutant and wild-type p53 promotes the formation of a p53/p73 complex that determines cell fate: apoptosis in the context of wild-type p53 or cell survival in the context of the mutant. These findings refine our current understanding of both the mechanistic links between p53 and p73 and the functional role for Thr^{81} phosphorylation.

Introduction

The transcription factor family comprising p53, p63, and p73 are critical regulators of cell fate, specifically through the induction of apoptotic cell death in response to cellular stress and developmental cues. The three proteins have distinct as well as overlapping and interdependent functions. Mutations in p53 are common in human tumors; gain-of-function p53 mutants have a dominant-negative effect on wild-type p73 by binding it and inhibiting its ability to bind DNA and thereby preventing its transcriptional induction of apoptotic gene (*1, 2*). In mice, knockout of one or both alleles of the individual genes encoding p53, p63, or p73 resulted in reduced cell death in response to DNA-damaging stimuli (*3*), indicating that all three proteins are necessary to invoke a robust apoptotic response in that context. However, whereas wild-type p63 and p73 form heterodimeric (or higher order) complexes, wild-type p53 reportedly does not (*4, 5*).

Wild-type p53 has two transactivation domains: TAD1 (amino acids 1-40) and TAD2 (amino acids 43-54). TAD2 is located proximal to the proline-rich domain (PRD; amino acids 63-97) (*6, 7*), and both TAD2 and the PRD are critical for p53's induction of apoptotic genes (*8, 9*), whereas TAD1 is reportedly dispensable for this function (*10*). Thr^{81} is a key phosphorylation site within the PRD, as is Ser^{46} within TAD2 (*11-15*). Several kinases reportedly phosphorylate Ser^{46} (*13, 16, 17*), and c-Jun N-

terminal kinase (JNK) phosphorylates Thr^{81} (*18*), yet precisely how modification of Thr^{81} regulates p53 activity in the context of apoptosis induction is limited.

The PRD is an important structural domain; prolyl isomerization in this domain regulates the structure of other domains of p53 (*19*). Additionally, the PRD is necessary for growth suppression and apoptosis (*20, 21*). We rationalized that phosphorylation within this domain may also be sufficient to alter the structure of other domains in p53 and thereby regulate its functional interactions. Our findings support previously published work on genetic knockout mice, the PRD, and mutant p53/p73 complex formation (*1, 2*) but refine our current understanding of the interaction between wild-type p53 and p73.

Results

The phosphorylation of p53 by JNK results in the induction of apoptotic protein PUMA

Because JNK is a key inducer of p53-mediated apoptosis, and JNK phosphorylates p53 at Thr^{81}, we were first curious whether Thr^{81} was phosphorylated in mutant p53 in cells. In MDA-MB-468 cells, which have a missense mutation in p53 (R273H^{R273X}), TMD231 cells, which have a missense mutation in p53 (R280KX), and MDA-MB-157 cells, which have a truncation mutation in p53 (A88fs*52) , JNK was activated, as determined by immunoblotting with antibodies against phospho-Tyr^{183}/Tyr^{185} JNK (Fig. 1A). In addition, mutant p53 was phosphorylated at Thr^{81} in cells cultured in growth-supporting conditions. Treatment with the DNA topoisomerase inhibitor camptothecin or the protein synthesis inhibitor anisomycin increased phosphorylation of JNK and phos-Thr^{81}. In various cells that have wild-type p53, namely untransformed cell lines NIH3T3 (mouse fibroblast) and HME1 (human mammary epithelial), as well as human foreskin fibroblast BJ cells and glioblastoma cell lines U87 and SF767, exhibited limited activation of JNK and phosphorylation of p53-Thr^{81} under growth conditions, but robust induction of both upon camptothecin or anisomycin exposure (Fig. 1B and fig. S1). Thus in “normal” cells and tumor cells, JNK is activated and p53 (wild-type or mutant) is phosphorylated at Thr^{81} in response to cell stress.

We then examined the dependence of JNK activation on the induction of *PUMA*, the apoptotic downstream target of p53. PUMA abundance was increased by anisomycin treatment in cells that had

wild-type p53 (Fig. 1C), but this induction was blocked by pretreatment with the small molecule JNK inhibitor SP600125, thereby confirming that activation of JNK was important for induction of the p53 target PUMA. Alongside this increase in PUMA abundance was a significant increase in cell death, thereby confirming the functional outcome of the pathway (fig. S2).

The predicted structure of a Thr^{81} phosphomimic shows a potential mode of binding to p73

To gain insight into the structural implications of phosphorylation at Thr^{81} of p53, we took advantage of a protein structure prediction algorithm, I-TASSER (Iterative Threading ASSEmbly Refinement) (*22-24*). Using I-TASSER, we generated predicted protein structure models for wild-type p53, R248W mutant p53 (a common DNA binding domain mutant), and a Thr^{81} phosphomimic p53 (T81E) (Fig. 2, and data files S1-S5). Analysis of wild-type and mutant p53 showed distinct structural differences in the amino and carboxy termini. The Thr^{81} phosphomimic mutation (T81E) substantially changed the structure of the tetramerization/regulatory (TET/REG) domain compared to that of the unphosphorylated wild-type p53. The TET/REG domain of the T81E model more closely resembled the R248W mutant p53 model than the wild-type p53 model. The R248W mutation of p53 is one of the mutants that binds to p73 (*1*). It is probable that it is this structural change in the TET/REG domain that enables p53 to interact with p73, which explains the original finding that wild-type p53 was unable to bind to p73. The results of our structural analysis implies that phosphorylation at Thr^{81} of p53 is permissive of binding to p73. We also produced in silico structural models of the S46D phosphomimic p53 and a R248W/T81E mutant p53 phosphomimic (Fig. 2) to examine if there were any structural changes in these constructs. The TAD2 of the S46D phosphomimic was structurally similar to the T81E phosphomimic but distinct from either of the R248W mutant p53 models. Given that phosphorylation at Ser^{46} of p53 is needed for a robust apoptotic response, and phosphorylation at Thr^{81} of p53 causes a structural change similar to that of phosphorylation at Ser^{46}, these data suggest that TAD2 and PRD are integrated into important structural changes that are associated with induction of apoptotic genes. Compared to mutant p53 alone (R248W), the Thr^{81} phosphomimic of R248W mutant p53 (R248W/T81E)

causes an additional structural change in almost every single functional domain. This finding would suggest that the use of a JNK inhibitor may reduce the binding of mutant p53 to p73 without completely ablating the interaction.

Phosphorylation of Thr^{81} of p53 promotes a p53-p73 complex

Our structural data (Fig. 2) combined with previous reports that mutant p53 binds wild-type p73 and the observation of high basal Thr^{81} phosphorylation of mutant p53 (Fig.1) led us to examine whether blocking JNK with the selective small-molecule inhibitor SP600125 could alter the mutant p53-p73 interaction endogenously. Mutant p53 was immunoprecipitated from lysates from TMD231 cells treated with DMSO or SP600125 and blotted for coincident pulldown of p73. We found that p73 co-purified with mutant p53 and that this binding was decreased by 40% when JNK activity was blocked with SP600125 (Fig. 3A). This data suggests that JNK has only a modest effect on the interaction between mutant p53 and p73, which was predicted in the structural data (Fig.2). We next tested whether wild-type p53 and p73 were affected by JNK-mediated phosphorylation. To do this, we transiently transfected H1299 cells with wild-type p53 and HA-tagged p73, then treated the transfected cells with DMSO or anisomycin. Immunoprecipitation of wild-type p53 from cellular extracts shows that p73 co-purified only when JNK was activated with anisomycin (Fig. 3B). To provide evidence that phosphorylation of Thr^{81} was necessary for wild-type p53 to co-purify with p73, we transiently transfected H1299 cells with wild-type p53 or the T81E phosphomimic. Immunoprecipitation of exogenous p53 revealed that T81E, but not wild-type p53, co-purified with endogenous p73 (Fig. 3C) Likewise, immunoprecipitation of endogenous p73 from extracts from U87 cells treated with DMSO, anisomycin, SP600125, or pretreated with SP600125 before anisomycin showed that endogenous wild-type p53 co-purifed with p73 only when Thr^{81} was phosphorylated (Fig. 3D). These data substantially suggest that Thr^{81} phosphorylation in p53 is critical for the formation of a wild-type p53-p73 complex. To definitively show this, we used various p53 phosphomimics (T81E, S46D, T81E-S46D) and p73 produced in bacteria and performed Far-Western analysis to examine the requirement of Thr^{81} phosphorylation. We fixed recombinant wild-type p53, the

phosphomimics, and two positive controls (MDM2 and MDMX) to nitrocellulose, then incubated the membrane with recombinant p73 and blotted for p73. In support of our cellular data presented above, this in vitro approach confirmed that p73 bound only to T81E and not wild-type p53 or S46D p53 (Fig. 3E). We also probed for p53 in a separate lane to show the relative amounts of p53 loaded per well (Fig. 3E). Collectively, through overexpression, endogenous and recombinant approaches, we conclude that p73 will bind to wild-type p53 when p53 is phosphorylated at Thr^{81}.

To gain insight into where p53 and p73 interact, we performed confocal immunofluorescence microscopy analysis on MDA157, HME, or TMD231 cells grown on coverslips and treated with anisomycin, SP600125, or DMSO. Anisomycin treatment caused a significant increase in colocalization between p53 and p73 in the nucleus of p53–wild-type HME cells but not p53-mutant MDA157 cells (Fig. 4, A and B; table S1). Blocking JNK activity with SP600125 in TMD231 cells, which have mutant p53 and high basal activation of JNK, caused a significant decrease in the colocalization of mutant p53 and p73 in the nucleus (Fig. 4C and table S1), which is in accordance with the decrease in binding of mutant p53 and p73 (Fig. 3). To ensure that anisomycin was indeed activating JNK and increasing phosphorylation at Thr^{81}, and that SP600125 was inhibiting JNK and decreasing phosphorylation at Thr^{81} of p53, the same cells were treated as described in the confocal experiments and lysates were Western blotted for active JNK and phosphorylated Thr^{81} p53 (fig. S3).

The JNK-initiated p53-p73 pathway is important for apoptosis

Above, we showed that phosphorylation of Thr^{81} of p53 resulted in its interaction with p73 (Fig. 3) and an increased abundance of PUMA (Fig. 1C). Therefore, we examined whether p53, p73, and JNK activation was necessary for the induction of apoptosis. We showed that the removal of p53 in p53–wild-type BJ cells resulted in resistance to JNK-activated cell death by anisomycin treatment (Fig. 5A). Specifically, treatment with anisomycin for 9 hours initiated a steady increase in the abundance of BAX and PUMA, which was prevented by shRNA-mediated knockdown of p53. In contrast, the abundance of

BAX increased after 6 hours of anisomycin treatment; this may be due to the cells overcoming the shRNA knockdown at 6 hours in response to prolonged anisomycin-induced stress (Fig. 5A).

The apoptotic resistance conferred to BJ cells transfected with p53-shRNA was further investigated using a methylene-blue cell death assay (Fig. 5B) and by assessing cell number as a factor of green fluorescent protein (GFP) (shRNA vector) signal (Fig. 5C). Loss of p53 improved cell viability through anisomycin treatment (Fig. 5, B and C), suggesting that the lack of the p53-p73 complex results in resistance to apoptosis. To test the impact of specifically Thr^{81} phosphorylation on cell death, we co-expressed GFP and either wild-type p53 or a p53 mutant that cannot be phosphorylated at Thr^{81} (T81A) in H1299 cells and examined survival after anisomycin treatment by GFP fluorescence. The data revealed an increase in survival in cells expressing T81A point mutation compared to wild-type p53 (Fig. 5D), confirming previously published observations with this mutant (*18*) and that Thr^{81} phosphorylation in p53 is critical to cell stress-induced apoptosis.

Discussion

The tumor suppressor p53 is highly studied given its role in regulating many cellular activities and responses, including cell cycle arrest, DNA repair, cell death, and metabolism. Its family member p73 has some described overlapping functions; yet, unlike p53, p73 is rarely mutated in human cancer. While p73 is rarely mutated, mutation of p53 may function as a dominant negative to ablate p73 activity (*1*). The regulation of p53 is extremely important given that its differential regulation can dictate distinct binding partners and, consequently, distinct outcomes through transcriptional targets, such *PTEN* to promote apoptosis versus *MDM2* to promote re-entry into the cell cycle and survival (*25, 26*). Increased abundance of PTEN, a protein/lipid phosphatase that inhibits the PI3K (phosphatidylinositol 3-kinase)–AKT (protein kinase B) pathway, can protect p53 from MDM2-mediated degradation induced by AKT (*11, 27-30*). Thus, p53 can selectively induce *PTEN* expression and programmed cell death instead of the autoregulatory feedback loop with MDM2 to promote cell survival (*11, 31*). Moreover, PTEN can form a

complex with p73 and bind to the *PUMA* promoter to increase its expression, leading to the induction of apoptosis (*32*). These molecular and biochemical studies are supported by genetic studies in mice where the loss of p53, p73, or PTEN confers resistance to apoptotic stimuli and an increase in neoplastic development (*3, 33-36*). Thus, an effective response to apoptotic stimuli requires the integration of numerous intact tumor suppressors, yet how these tumor suppressors are signaled to form a complex has not previously been clearly defined.

There are well-characterized kinase signaling pathways that phosphorylate p53 and p73 in response to DNA damage, but some phosphorylation sites appear to be dispensable for the induction of apoptosis. It has been reported by several groups that Ser^{46} and Thr^{81} are important for the induction of apoptosis (*11, 13, 15, 17*). Homeodomain-interacting protein kinase 2 (HIPK2) and the mitogen-activated protein kinase p38 reportedly phosphorylate Ser^{46} of p53, whereas JNK, which plays dual roles in cellular proliferation and cell death (*37*), phosphorylates Thr^{81} of p53 (*11, 13, 15, 17*). One of JNK's substrates is p73, which mediates JNK-induced apoptosis (*38*), but it was unclear how. Analysis of apoptosis by the JNK-p73 axis in that previous study (*38*) was performed in cells that maintained expression of wild-type p53, and notably, p53 abundance does not directly correlate with its activity; for example, neddylation of p53 in response to growth factor signaling renders p53 stable but inactive (*39*). Untransformed cell lines have an intact apoptotic pathway and deneddylating enzymes, tumor suppressors, active kinases, and post-translational modification enzymes that are activated in response to genotoxic stress that provide a robust induction of apoptosis.

There is renewed interest in p53 family member interactions, and several studies have highlighted the importance of the interactions between different family members (*40-42*). Our studies have linked the JNK-p53-p73 proteins showing that phosphorylation of p53 at Thr^{81} by JNK is permissive of a p53-p73 interaction. Notably, our structural modeling analysis revealed that the structure of phosphorylated Thr^{81} is nearly identical to that of R248W. Therefore, activated JNK can convert wild-type p53 to mimic mutant p53 with regards to binding to p73 by exposing the DNA binding domain. Ser^{46} is proximal to the proline

rich domain in the second transactivation domain, which may be important for additional structural changes to recruit other factors for gene expression. However, we also found that phosphorylation of Ser^{46} has no effect on binding to p73, supporting that this phosphorylation may instead be required for recruiting additional coactivators. The JNK-mediated interaction between wild-type p53 and p73 provides biochemical evidence in support of the existing animal models and gene dose sensitivity of p53 and p73 to apoptosis (*33*). We also show that in mutant p53 cells, JNK activity is increased resulting in a mutant p53/wild-type p73 complex with mutant p53 acting as a dominant negative partner of p73. These data are consistent with previous reports showing that mutant p53/p73 form a complex (*2*). This complex mediates apoptosis in cells that express wild-type p53, but survival in cells that express mutant p53. Thus, our findings refine our understanding of how cells promote, or in certain contexts circumvent, the p53 apoptotic signaling axis.

Materials and Methods

*Cell culture and transfection***.** H1299, TMD231, U87, HME1, SF767, 3T3, hTert BJ, MDA-MB-468 and MDA-MB-157 were cultured in Dulbecco's Modified Eagle Media (DMEM) with 10% fetal bovine serum (FBS) supplemented with penicillin and streptomycin at 37^0 C humidified incubator in 5% CO_2. Anisomycin, SP600125, and Camptothecin were purchased and suspended as described by the manufacturer (Sigma-Aldrich). Anisomycin was used at 30 μM, Camptothecin was used at 30 μM, and SP600125 was used at 25 μM unless otherwise noted. Transient transfections were performed using lipofectamine per manufacturer's instructions (Life Technologies). Annexin V cell dead kit from Millipore was used to stain cells which were analyzed on a MUSE cytometer.

Plasmids, protein purification, and Western blotting. We generated mutant p53 at Thr^{81} with a site directed mutagenesis kit (Life technologies). Recombinant p73 and p53 proteins were produced in

BL21DE3 cells and purified as previously described (*30, 32*). Far-Western was completed by 96-well dot blot system and recombinant proteins were placed in wells and fixed to nitrocellulose by drying. Blot was blocked with 5% nonfat dry milk and incubated with recombinant p73. p73 was then detected by p73 antibody followed by secondary and an enhanced chemiluminescence (ECL) reagent. Western blot analysis used whole cell lysates lysed under denaturing conditions (6 M urea buffer) or immunoprecipitated proteins extracted with lysis buffer, as described previously (*32*). Antibody for p73 (OP1008) was purchased from Millipore; antibodies for phos-T81, phos-Y183/Y185 JNK, and PUMA were purchased from Cell Signaling Technology; and antibodies for p53 (D0-1), actin, and GAPDH were purchased from Santa Cruz Biotechnology.

I-TASSER protein structure prediction. Amino acid sequences for wild-type p53, R248W p53, T81E p53, S46D, and R248W/T81E p53 were input to the I-TASSER web server as FASTA sequences. Predicted protein structures were generated using a previously described method (*22-24*) and analyzed using the CCP4 Molecular Graphics Program (CCP4MG) v. 2.10.6 (*43*). Structures were superposed using a built-in function within the software.

Immunofluorescence microscopy. MDA157, HME, or TMD231 cells were grown on glass coverslips and fixed in 4% paraformaldehyde in phospho-buffered saline (PBS) for 15 minutes, washed with PBS, and permeabilized in 1% Triton X-100 in PBS for 15 minutes. Coverslips were blocked in 5% bovine serum albumin for 1 hour in PBS/Tween before being stained with p73 (D3G10, rabbit monoclonal, Cell Signaling Technologies) and p53 (DO-1, mouse monoclonal, Santa Cruz) antibodies. Coverslips were then incubated with anti-rabbit AlexaFluor 647 and anti-mouse AlexaFluor 488 secondary antibodies before being fixed to slides with ProLong Diamond Antifade Mountant with DAPI (Life Technologies). Slides were visualized on a Leica SP8 MP microscope. Colocolization analysis was performed using Imaris v9.0.2, and colocalized images were created using the "RG2B_Colocolization" plugin for ImageJ. Scale bar, 25 μm (MDA157, TMD231) or 50 μm (HME).

Colony forming assay. Empty vector- or shp53-transduced hTert BJ cells where plated in triplicate and treated with anisomycin for 9 hours. Dimethyl sulfoxide (DMSO) was used as a vehicle control. Cells were stained with equal parts methanol and methylene blue for 15 min. The plate was then washed 3 times with deionized water to remove any excess stain and left to dry at room temperature.

GFP florescence assay. BJ cells expressing green fluorescent protein (GFP) *TP53* shRNA (shp53) or empty (control) pLVTHM vector (XXXX) were plated in quadruplet and treated with DMSO or anisomycin (10 μM) for 48 hours. Fluorescence emitted by GFP in each well was measured at 509 nm using a SpectraMax M5 spectrophotometer (Molecular Devices).

Statistical analysis. Data were analyzed by two-tailed unpaired t tests. P values <0.05 were considered significant.

Supplementary Materials

Figure S1. Phosphorylation of Thr^{81} in cell lines with wild-type p53.
Figure S2. U87 cell death.
Figure S3. JNK activation or inhibition in HME, MDA157, and TMD231 cell lines.
Table S1. Manders' Coefficients for microscopy colocalization analysis .
Data File S1. Wild-type p53 structure (PDB).
Data File S2. p53 R248W structure (PDB).
Data File S3. p53 T81E structure (PDB).
Data File S4. p53 S46D structure (PDB).

Data File S5. p53 R248W/T81E structure (PDB).

References and Notes:

1. C. J. Di Como, C. Gaiddon, C. Prives, p73 function is inhibited by tumor-derived p53 mutants in mammalian cells. *Mol Cell Biol* **19**, 1438-1449 (1999).
2. C. Gaiddon, M. Lokshin, J. Ahn, T. Zhang, C. Prives, A subset of tumor-derived mutant forms of p53 down-regulate p63 and p73 through a direct interaction with the p53 core domain. *Mol Cell Biol* **21**, 1874-1887 (2001).
3. E. R. Flores *et al.*, Tumor predisposition in mice mutant for p63 and p73: evidence for broader tumor suppressor functions for the p53 family. *Cancer Cell* **7**, 363-373 (2005).
4. T. S. Davison *et al.*, p73 and p63 are homotetramers capable of weak heterotypic interactions with each other but not with p53. *J Biol Chem* **274**, 18709-18714 (1999).
5. A. C. Joerger *et al.*, Structural evolution of p53, p63, and p73: implication for heterotetramer formation. *Proc Natl Acad Sci U S A* **106**, 17705-17710 (2009).
6. J. Zhu, J. Jiang, W. Zhou, K. Zhu, X. Chen, Differential regulation of cellular target genes by p53 devoid of the PXXP motifs with impaired apoptotic activity. *Oncogene* **18**, 2149-2155 (1999).
7. J. Zhu, S. Zhang, J. Jiang, X. Chen, Definition of the p53 functional domains necessary for inducing apoptosis. *J Biol Chem* **275**, 39927-39934 (2000).
8. E. M. Ruaro *et al.*, A proline-rich motif in p53 is required for transactivation-independent growth arrest as induced by Gas1. *Proc Natl Acad Sci U S A* **94**, 4675-4680 (1997).
9. C. Venot *et al.*, The requirement for the p53 proline-rich functional domain for mediation of apoptosis is correlated with specific PIG3 gene transactivation and with transcriptional repression. *EMBO J* **17**, 4668-4679 (1998).
10. J. Zhu, W. Zhou, J. Jiang, X. Chen, Identification of a novel p53 functional domain that is necessary for mediating apoptosis. *J Biol Chem* **273**, 13030-13036 (1998).
11. L. D. Mayo *et al.*, Phosphorylation of human p53 at serine 46 determines promoter selection and whether apoptosis is attenuated or amplified. *J Biol Chem* **280**, 25953-25959 (2005).
12. Y. Wang, K. M. Debatin, H. Hug, HIPK2 overexpression leads to stabilization of p53 protein and increased p53 transcriptional activity by decreasing Mdm2 protein levels. *BMC Mol Biol* **2**, 8 (2001).
13. G. D'Orazi *et al.*, Homeodomain-interacting protein kinase-2 phosphorylates p53 at Ser 46 and mediates apoptosis. *Nat Cell Biol* **4**, 11-19 (2002).
14. T. G. Hofmann *et al.*, Regulation of p53 activity by its interaction with homeodomain-interacting protein kinase-2. *Nat Cell Biol* **4**, 1-10 (2002).
15. S. Y. Fuchs, V. Adler, M. R. Pincus, Z. Ronai, MEKK1/JNK signaling stabilizes and activates p53. *Proc Natl Acad Sci U S A* **95**, 10541-10546 (1998).
16. S. Saito *et al.*, ATM mediates phosphorylation at multiple p53 sites, including Ser(46), in response to ionizing radiation. *J Biol Chem* **277**, 12491-12494 (2002).
17. D. V. Bulavin *et al.*, Phosphorylation of human p53 by p38 kinase coordinates N-terminal phosphorylation and apoptosis in response to UV radiation. *EMBO J* **18**, 6845-6854 (1999).
18. T. Buschmann *et al.*, Jun NH2-terminal kinase phosphorylation of p53 on Thr-81 is important for p53 stabilization and transcriptional activities in response to stress. *Mol Cell Biol* **21**, 2743-2754 (2001).
19. M. Berger, N. Stahl, G. Del Sal, Y. Haupt, Mutations in proline 82 of p53 impair its activation by Pin1 and Chk2 in response to DNA damage. *Mol Cell Biol* **25**, 5380-5388 (2005).
20. K. K. Walker, A. J. Levine, Identification of a novel p53 functional domain that is necessary for efficient growth suppression. *Proc Natl Acad Sci U S A* **93**, 15335-15340 (1996).
21. N. Baptiste, P. Friedlander, X. Chen, C. Prives, The proline-rich domain of p53 is required for cooperation with anti-neoplastic agents to promote apoptosis of tumor cells. *Oncogene* **21**, 9-21 (2002).
22. A. Roy, A. Kucukural, Y. Zhang, I-TASSER: a unified platform for automated protein structure and function prediction. *Nat Protoc* **5**, 725-738 (2010).
23. J. Yang *et al.*, The I-TASSER Suite: protein structure and function prediction. *Nat Methods* **12**, 7-8 (2015).
24. Y. Zhang, I-TASSER server for protein 3D structure prediction. *BMC Bioinformatics* **9**, 40 (2008).

25. L. D. Mayo, J. E. Dixon, D. L. Durden, N. K. Tonks, D. B. Donner, PTEN protects p53 from Mdm2 and sensitizes cancer cells to chemotherapy. *J Biol Chem* **277**, 5484-5489 (2002).
26. V. Stambolic *et al.*, Regulation of PTEN transcription by p53. *Mol Cell* **8**, 317-325 (2001).
27. J. A. Eitel *et al.*, PTEN and p53 are required for hypoxia induced expression of maspin in glioblastoma cells. *Cell Cycle* **8**, 896-901 (2009).
28. L. D. Mayo, D. B. Donner, A phosphatidylinositol 3-kinase/Akt pathway promotes translocation of Mdm2 from the cytoplasm to the nucleus. *Proc Natl Acad Sci U S A* **98**, 11598-11603 (2001).
29. A. G. Li *et al.*, Mechanistic insights into maintenance of high p53 acetylation by PTEN. *Mol Cell* **23**, 575-587 (2006).
30. T. Maehama, J. E. Dixon, PTEN: a tumour suppressor that functions as a phospholipid phosphatase. *Trends Cell Biol* **9**, 125-128 (1999).
31. X. Wu, J. H. Bayle, D. Olson, A. J. Levine, The p53-mdm-2 autoregulatory feedback loop. *Genes Dev* **7**, 1126-1132 (1993).
32. J. A. Lehman *et al.*, Induction of apoptotic genes by a p73-phosphatase and tensin homolog (p73-PTEN) protein complex in response to genotoxic stress. *J Biol Chem* **286**, 36631-36640 (2011).
33. E. R. Flores *et al.*, p63 and p73 are required for p53-dependent apoptosis in response to DNA damage. *Nature* **416**, 560-564 (2002).
34. F. Talos, A. Nemajerova, E. R. Flores, O. Petrenko, U. M. Moll, p73 suppresses polyploidy and aneuploidy in the absence of functional p53. *Mol Cell* **27**, 647-659 (2007).
35. A. Di Cristofano, B. Pesce, C. Cordon-Cardo, P. P. Pandolfi, Pten is essential for embryonic development and tumour suppression. *Nat Genet* **19**, 348-355 (1998).
36. A. Suzuki *et al.*, High cancer susceptibility and embryonic lethality associated with mutation of the PTEN tumor suppressor gene in mice. *Curr Biol* **8**, 1169-1178 (1998).
37. R. J. Davis, Signal transduction by the c-Jun N-terminal kinase. *Biochem Soc Symp* **64**, 1-12 (1999).
38. E. V. Jones, M. J. Dickman, A. J. Whitmarsh, Regulation of p73-mediated apoptosis by c-Jun N-terminal kinase. *Biochem J* **405**, 617-623 (2007).
39. C. N. Batuello, P. M. Hauck, J. M. Gendron, J. A. Lehman, L. D. Mayo, Src phosphorylation converts Mdm2 from a ubiquitinating to a neddylating E3 ligase. *Proc Natl Acad Sci U S A* **112**, 1749-1754 (2015).
40. S. Kehrloesser *et al.*, Intrinsic aggregation propensity of the p63 and p73 TI domains correlates with p53R175H interaction and suggests further significance of aggregation events in the p53 family. *Cell Death Differ* **23**, 1952-1960 (2016).
41. J. Gebel *et al.*, Mechanism of TAp73 inhibition by DeltaNp63 and structural basis of p63/p73 hetero-tetramerization. *Cell Death Differ* **23**, 1930-1940 (2016).
42. G. Chillemi *et al.*, Structural Evolution and Dynamics of the p53 Proteins. *Cold Spring Harb Perspect Med* **7**, (2017).
43. S. McNicholas, E. Potterton, K. S. Wilson, M. E. Noble, Presenting your structures: the CCP4mg molecular-graphics software. *Acta Crystallogr D Biol Crystallogr* **67**, 386-394 (2011).

Acknowledgments: We would like to thank members of the Mayo laboratory for critical reading of the manuscript. Phil Wubbolding and Paula M. Hauck for production and purification of recombinant proteins. **Funding**: This work was supported in part through funds provided by: the Jeff Gordon Children's Foundation, the Riley Children's Foundation, and NIH CA172256 to L.D.M. **Author contributions**: Experiments were performed and analyzed by E.R.W. and C.M.A. (contributed equally) and K.B. and A.B. (contributed equally). L.D.M. conducted some experiments and wrote the article. **Competing interests**: The authors declare that they have no

competing interests. **Data and materials availability:** All data needed to evaluate the conclusions in the paper are present in the paper or the Supplementary Materials.

Figure Legends:

Fig. 1. Phosphorylation of Thr^{81} of p53 in response to JNK activation. (A) Western blot of phosphorylated JNK, phosphorylated Thr^{81} of p53, and actin in cellular extracts from TMD231, MDA-MB-468 and MDA-MB-157 cells treated with either camptothecin or anisomycin for the indicated times. Blots are representative of three independent experiments. **(B)** Western Blot of phosphorylated JNK or Thr^{81} of p53 and actin from cellular extracts from 3T3, SF767, HME-1, BJ and U87 treated with anisomycin or camptothecin for the indicated times. Blots are representative of three independent experiments (quantified in fig. S1). **(C)** U87 or SF767 cellular extracts from DMSO, SP600125, anisomycin or pretreatment with SP600125 then anisomycin, and western blotted for PUMA and actin. Blots are representative of two independent experiments.

Fig. 2. Predicted structure for a Thr^{81} phosphomimic reveals a possible mode of binding to p73. (A and B) Structures (A) and amino acid coverage (B) of domains in wild-type and mutant p53. Whole protein represents amino acids 1-393 of p53. Transactivation domains 1 and 2 (TAD1/TAD2) represent amino acids 1-40 and 43-54. The proline rich domain (PRD) represents amino acids 63-97. The tetramerization and regulatory domains (TET/REG) represent amino acids 323-393. T81, Thr^{81}; E, glutamic acid in T81E phosphomimic mutant domain. Arrows in the TET/REG domain structures indicate the region of a conformational change that is permissive of binding.

Fig. 3. Formation and activity of a p53-p73 complex. (A) Immunoprecipitiation of p53 or control IgG from TMD231 cells treated with DMSO or SP600125 and western blotted for p73 and p53. Blots are

representative of four independent experiments. **(B)** Transient transfection of H1299 cells with p53, HA-p73 and treated with either DMSO or Anisomycin. Western blot of p53 and HA from p53 immunoprecipitated from cellular extracts. Blots are representative of two independent experiments. **(C)** Immunoprecipitiation of p53 or control IgG and western blot of p53 and p73 from H1299 cells transfected with wild type p53 or T81Ep53. WCL is whole cell lysate from H1299 cells. Blots are representative of two independent experiments. **(D)** Immunoprecipitation of endogenous p73 from U87 cells treated with SP600125, anisomycin or both and western blot of phospho-Thr^{81}, p53, and p73. Blots are representative of two independent experiments. **(E)** Far-Western analysis of p73 binding to p53. Lane 1 corresponds to p53 and the phosphomimics of p53; lane 2 is MDM2 and MDMX. Right, blotting for p73 to detect binding to p53, MDM2, and MDMX (right panel). Left, the relative amount of p53 on the membrane. Blots are representative of two independent experiments.

Fig. 4. Colocalization of p53 with p73. (A to C) Immunofluorescence assessing nuclear colocalization of p53 (green) and p73 (red) in MDA157 cells (A) and HME cells (B) treated with anisomycin (Aniso) or DMSO and in TMD231 cells (C) treated with SP600125 or DMSO. Arrows indicate the cell magnified in inset (bottom right) of each image. Scale bars, 25 μm (MDA157, TMD231) or 50 μm (HME). Data are mean ± S.E. from three independent experiments; *P* determined by two-tailed unpaired t test.

Fig. 5. Downstream effects of the p53-p73 pathway. (A) Western blot of BAX, PUMA, and p53 in cellular extracts from BJ cells transfected with empty vector control (E.V.) or p53-shRNA (shp53) and treated with anisomycin for the indicated time. Blots are representative of three independent experiments; E.V. and shp53 samples were developed on the same membrane. **(B)** Methylene Blue staining cell viability assay in E.V.- and shp53-transfected BJ cells treated with DMSO or anisomycin for 9 hours. Data is representative of three independent experiments. **(C)** Relative GFP fluorescence was measured in GFP shp53 and LVTHM empty vector BJ cells. Cells were treated with DMSO or anisomycin for 48 hours. Relative fluorescence was derived from DMSO controls. Data is representative of four independent

experiments. Significance was determined by a two-tailed unpaired t test (***P<0.005) (**D**) Green fluorescence was measured in H1299 cells transfected with GFP alone or GFP and either wild-type or T81A p53, then treated with DMSO or anisomycin. Fold change survival was calculated as the change in survival of anisomycin-treated cells relative to DMSO-treated cells, and normalized to the GFP-alone control. Data are mean ± S.E. from three independent experiments.

Fig. 6. Cell fate is dictated by formation of a p53-p73 complex. Schematic of our model. Apoptotic stimuli, for example DNA damage, results in the phosphorylation and activation of JNK. JNK phosphorylates wild-type p53 (green hexagons) at Thr^{81} causing a structural change in p53 and the subsequent binding of p73 (red diamonds). This complex drives the transcription of *PUMA* and *BAX*, leading to apoptosis. Mutant p53 (blue hexagons) does not require phosphorylation by JNK to form a complex with p73. Phosphorylation of mutant p53 instead serves to enhance p53 binding with p73, hence increasing total complex formation. However, because of the dysfunctional DNA binding domain in mutant p53 as well as its sequestering of p73 by complex formation, *PUMA* and *BAX* are not transcribed, thus decreasing the apoptotic signal and promoting tumor cell survival.

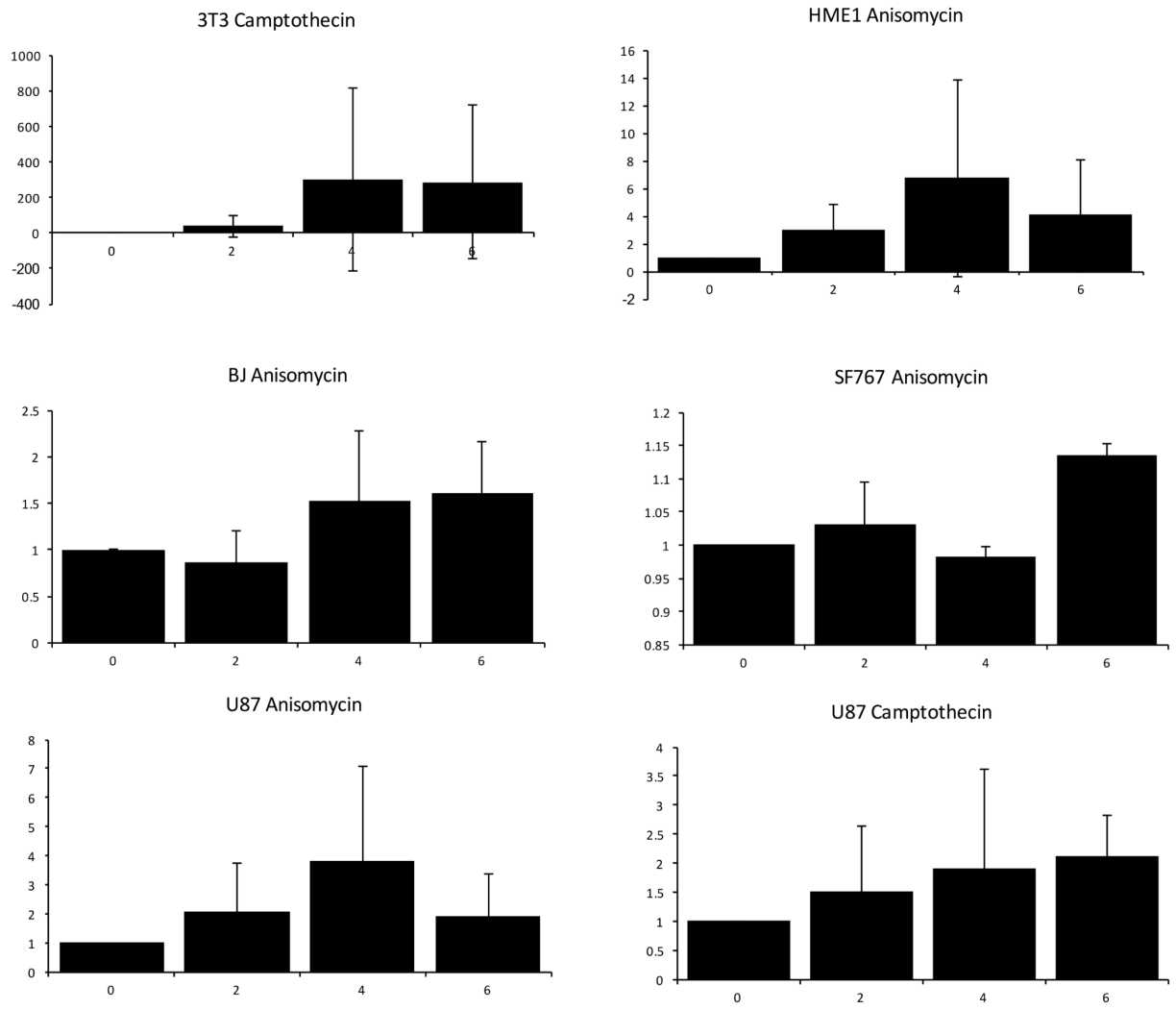

Figure S1. Activation of pT81 in WT p53 cell lines. Densitometry of pT81 p53 from three independent experiments plotted as the mean of the fold change +/- standard deviation.

Figure S2. U87 cell death. U87 cells were treated with 30 μM camptothecin for 6 hours or pretreated with 25 μM SP600125 for one hour and then treated with 30 μM camptothecin for 6 hours. Cell death was determined by flow cytometry using Annexin V. Error bars represent standard deviation from the mean; *P* values determined by a two-tailed unpaired t-test.

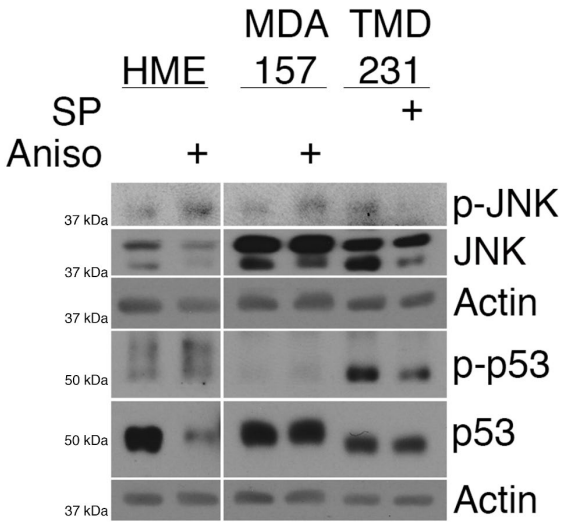

Figure S3. JNK activation or inhibition in HME, MDA157, and TMD231 cell lines. Western blotting for activated JNK (p-JNK) and phosphorylated p53 (at Thr^{81}; p-p53) in whole-cell lysates from HME and MDA157 cells treated with 30 μM anisomycin or DMSO for 6 hours and TMD231 cells treated with 25 μM SP600125 or DMSO for 6 hours.

	A = p73, B = p53	Manders' A	Standard Error	Manders' B	Standard Error
MDA157	DMSO (n = 109)	0.468	0.021	0.389	0.021
	Anisomycin (n = 61)	0.458	0.023	0.448	0.018
	Significance (p value)	0.763		0.060	
TMD231	DMSO (n = 53)	0.353	0.020	0.404	0.018
	SP600125 (n= 49)	0.114	0.012	0.398	0.009
	Significance (p value)	7.84E-17		0.765	
HME	DMSO (n = 72)	0.519	0.006	0.281	0.017
	Anisomycin (n = 67)	0.560	0.011	0.371	0.024
	Significance (p value)	0.001		0.002	

Table S1. Manders' Coefficients for microscopy colocalization analysis. Mander's A and B coefficients were generated using p73 as channel A and p53 as channel B within the Imaris software. Significance was determined using a two-tailed unpaired *t* test.

Data File S1. Wild-type p53 structure (PDB). Structure obtained from the I-TASSER software using the FASTA protein sequence for p53. NCBI Reference Sequence: NP_000537.3. Note: 3D Protein structure .pdb files require special software to view them. There is a web-based 3D structure viewer sponsored by NCBI (https://www.ncbi.nlm.nih.gov/guide/howto/view-3d-struct-prot/) that allows the user to upload and view .pdb files.

Data File S2. p53 R248W structure (PDB). Structure obtained from the I-TASSER software using the NCBI protein sequence for p53, with the addition of the R248W mutation. Note: 3D Protein structure .pdb files require special software to view them. There is a web-based 3D structure viewer sponsored by NCBI (https://www.ncbi.nlm.nih.gov/guide/howto/view-3d-struct-prot/) that allows the user to upload and view .pdb files.

Data File S3. p53 T81E structure (PDB). Structure obtained from the I-TASSER software using the NCBI protein sequence for p53, with the addition of the T81E mutation. Note: 3D Protein structure .pdb files require special software to view them. There is a web-based 3D structure viewer sponsored by NCBI (https://www.ncbi.nlm.nih.gov/guide/howto/view-3d-struct-prot/) that allows the user to upload and view .pdb files.

Data File S4. p53 S46D structure (PDB). Structure obtained from the I-TASSER software using the NCBI protein sequence for p53, with the addition of the S46D mutation. Note: 3D Protein structure .pdb files require special software to view them. There is a web-based 3D structure viewer sponsored by NCBI (https://www.ncbi.nlm.nih.gov/guide/howto/view-3d-struct-prot/) that allows the user to upload and view .pdb files.

Data File S5. p53 R248W/T81E structure (PDB). Structure obtained from the I-TASSER software using the NCBI protein sequence for p53, with the addition of both the R248W and the T81E mutations. Note: 3D Protein structure .pdb files require special software to view them. There is a web-based 3D structure viewer sponsored by NCBI (https://www.ncbi.nlm.nih.gov/guide/howto/view-3d-struct-prot/) that allows the user to upload and view .pdb files.

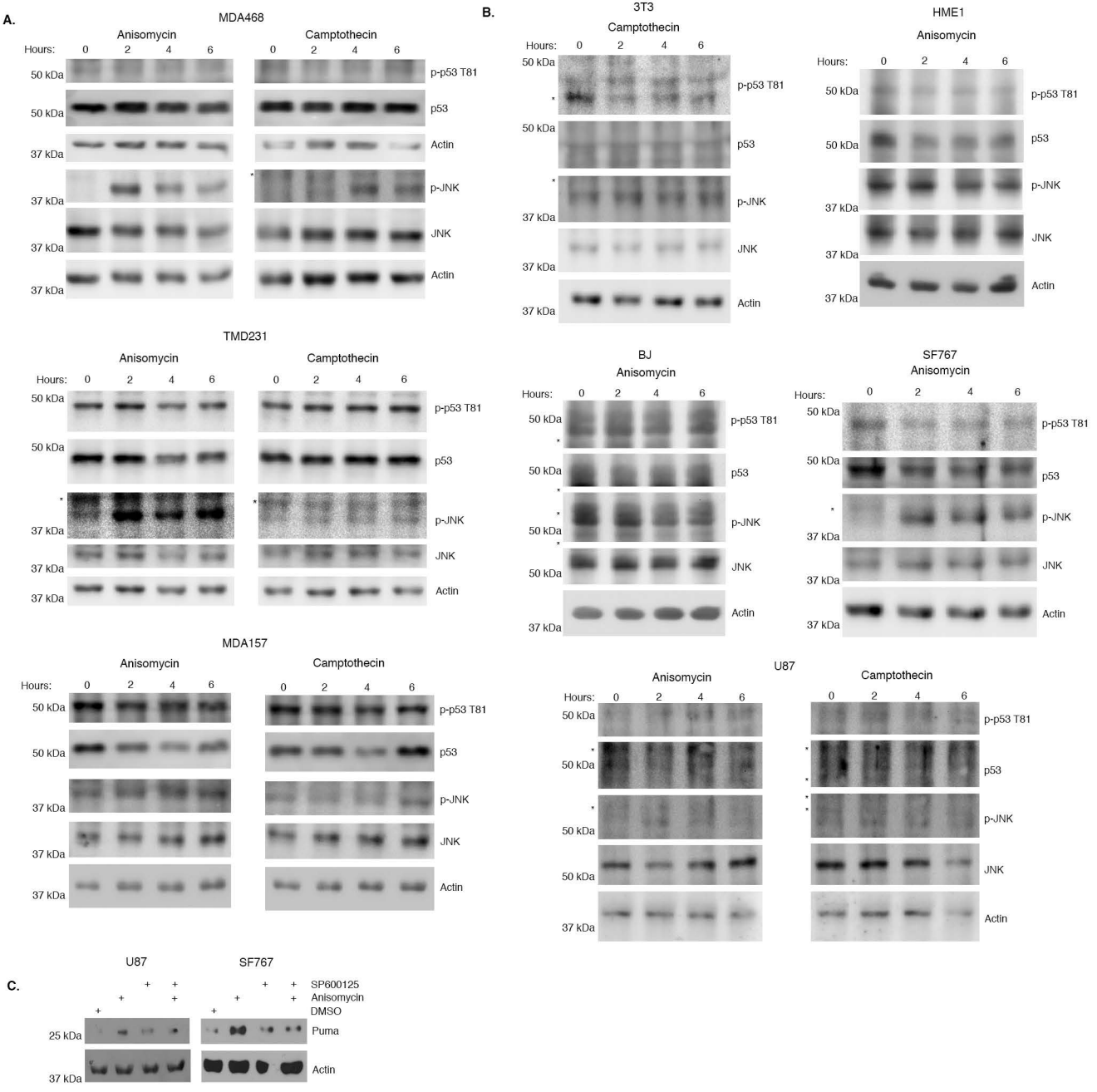
A.
MDA468
Anisomycin
Camptothecin
Hours: 0 2 4 6 0 2 4 6
50 kDa
p-p53 T81
p53
Actin
37 kDa
p-JNK
JNK
TMD231
MDA157
B.
3T3
Camptothecin
HME1
Anisomycin
BJ
SF767
U87
C.
U87
SF767
SP600125
Anisomycin
DMSO
25 kDa
Puma
37 kDa
Actin

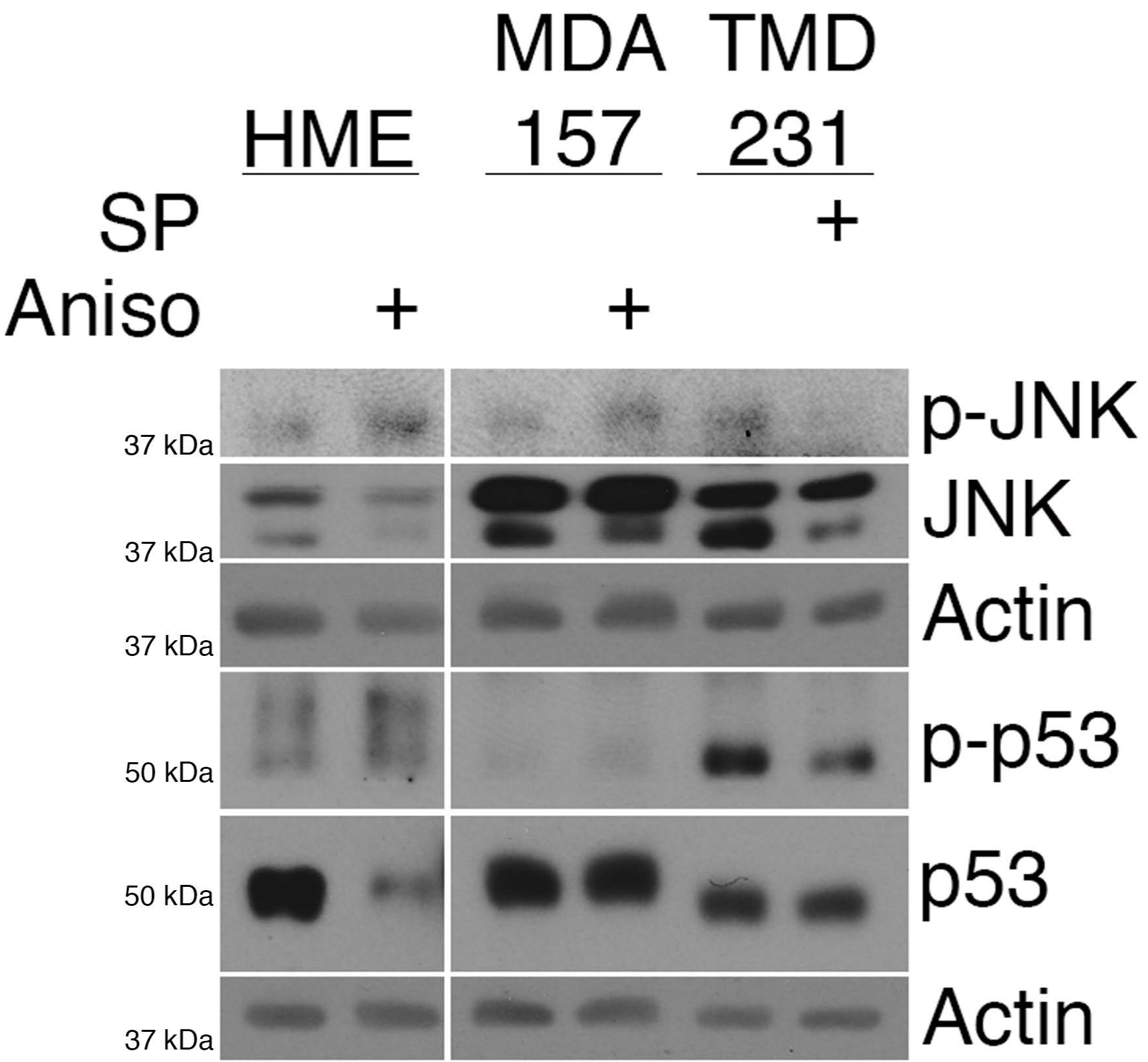
MDA
TMD
HME
157
231
SP
+
Aniso
+
+
37 kDa
37 kDa
37 kDa
50 kDa
50 kDa
37 kDa
p-JNK
JNK
Actin
p-p53
p53
Actin

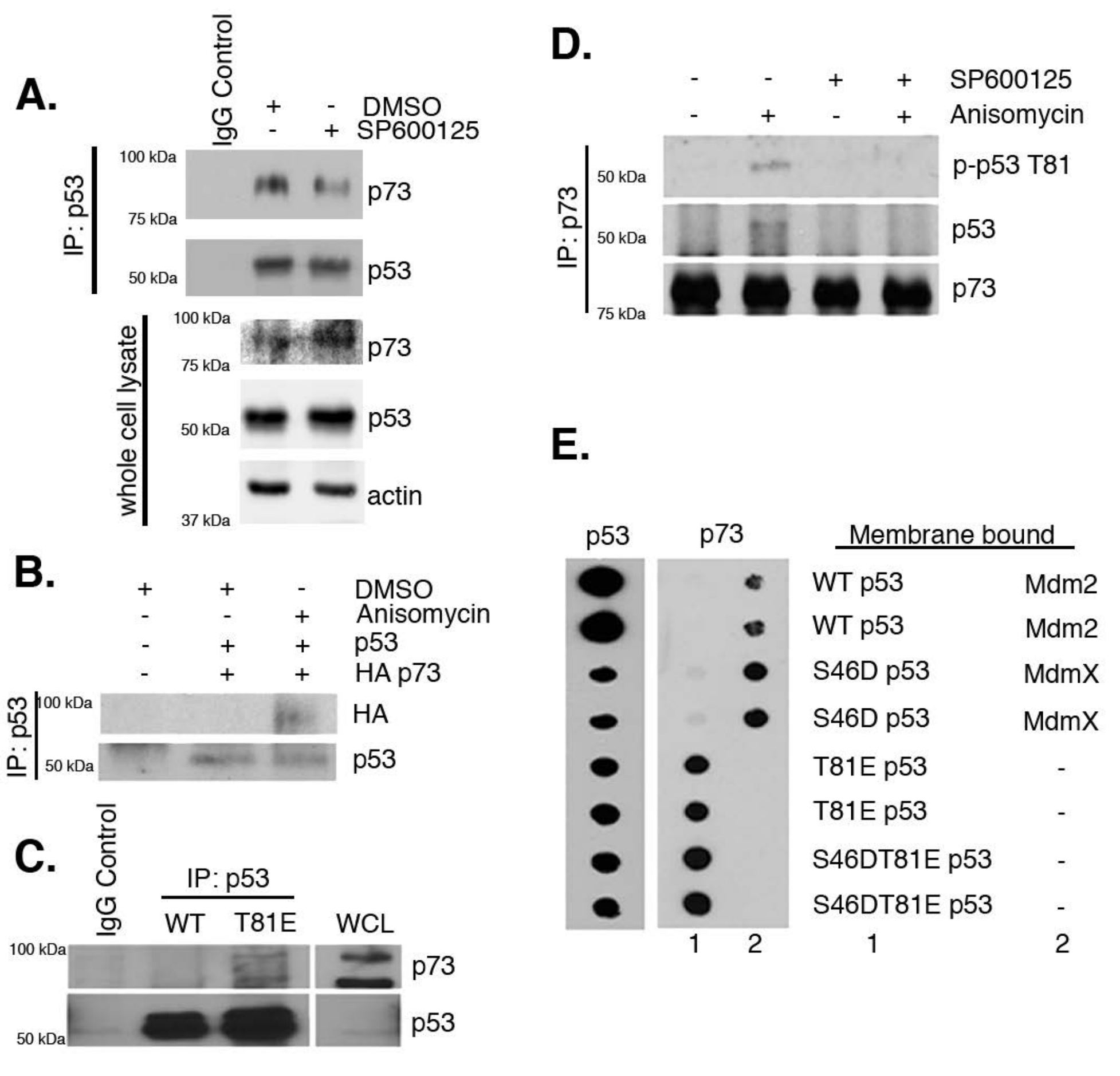
A.
IgG Control
+ - DMSO
- + SP600125
IP: p53
100 kDa
75 kDa
p73
50 kDa
p53
whole cell lysate
100 kDa
75 kDa
p73
50 kDa
p53
37 kDa
actin
B.
+ + - DMSO
- - + Anisomycin
- + + p53
- + + HA p73
IP: p53
100 kDa
HA
50 kDa
p53
C.
IgG Control
IP: p53
WT T81E
WCL
100 kDa
p73
50 kDa
p53
D.
- - + + SP600125
- + - + Anisomycin
IP: p73
50 kDa
p-p53 T81
50 kDa
p53
75 kDa
p73
E.
p53
p73
Membrane bound
WT p53 Mdm2
WT p53 Mdm2
S46D p53 MdmX
S46D p53 MdmX
T81E p53 -
T81E p53 -
S46DT81E p53 -
S46DT81E p53 -
1 2
1 2

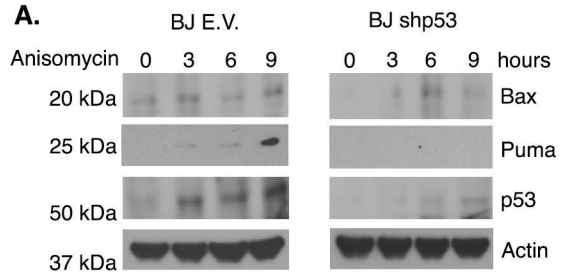
A.
BJ E.V.
BJ shp53
Anisomycin
0 3 6 9
0 3 6 9 hours
20 kDa
25 kDa
50 kDa
37 kDa
Bax
Puma
p53
Actin

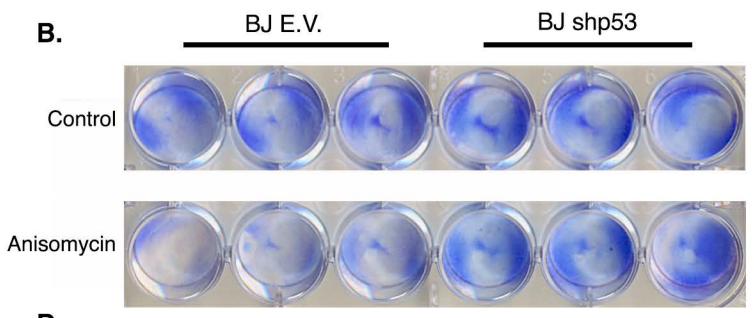
B.
BJ E.V.
BJ shp53
Control
Anisomycin

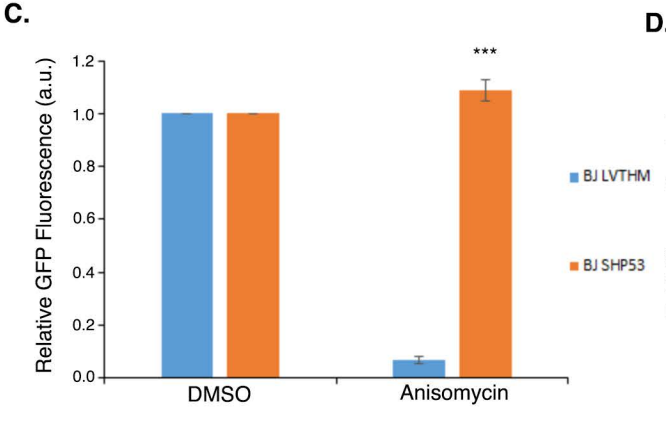
C.
Relative GFP Fluorescence (a.u.)
1.2
1.0
0.8
0.6
0.4
0.2
0.0
***
BJ LVTHM
BJ SHP53
DMSO
Anisomycin

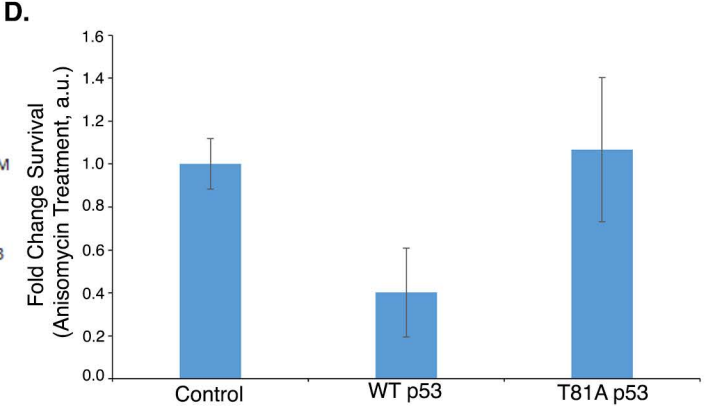
D.
Fold Change Survival
(Anisomycin Treatment, a.u.)
1.6
1.4
1.2
1.0
0.8
0.6
0.4
0.2
0.0
Control
WT p53
T81A p53

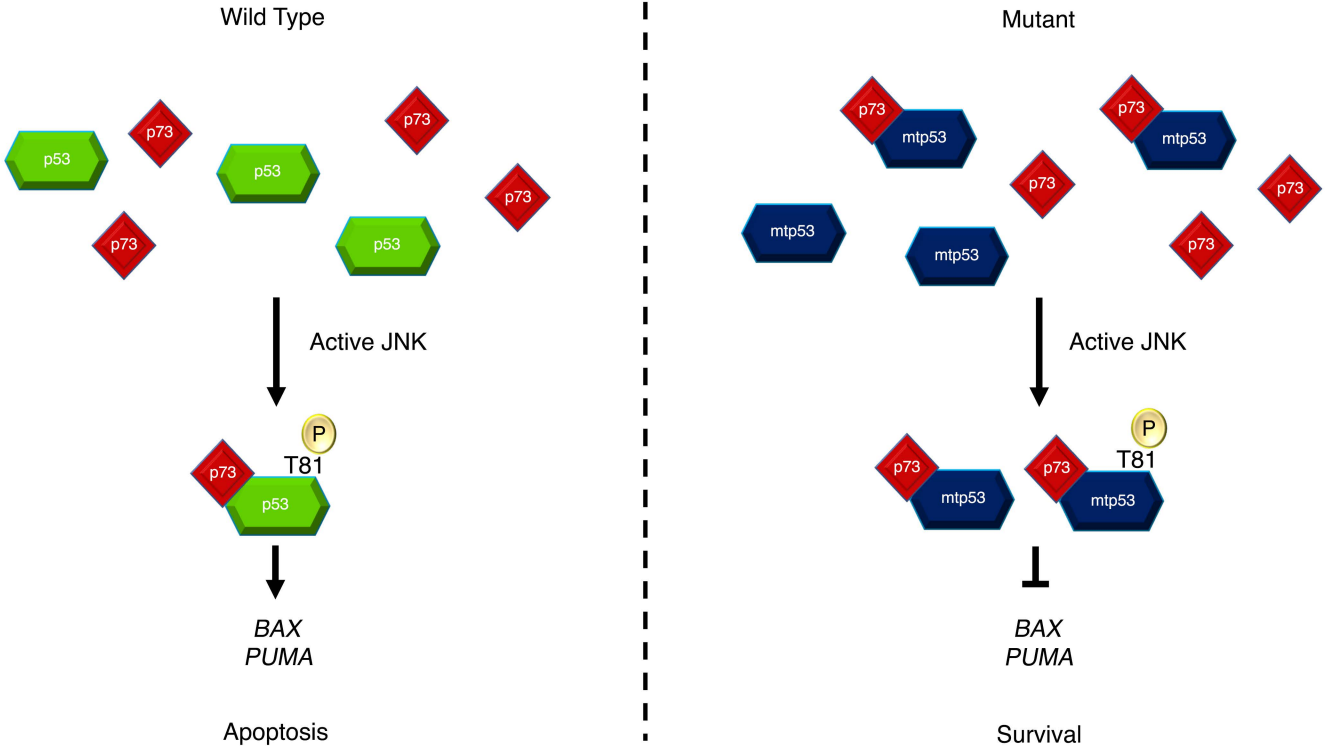
Wild Type
p53
p73
p53
p73
p73
p53
p73
Active JNK
P
T81
p73
p53
BAX
PUMA
Apoptosis
Mutant
p73
mtp53
p73
mtp53
p73
mtp53
mtp53
p73
Active JNK
P
T81
p73
mtp53
p73
mtp53
BAX
PUMA
Survival

3T3 Camptothecin

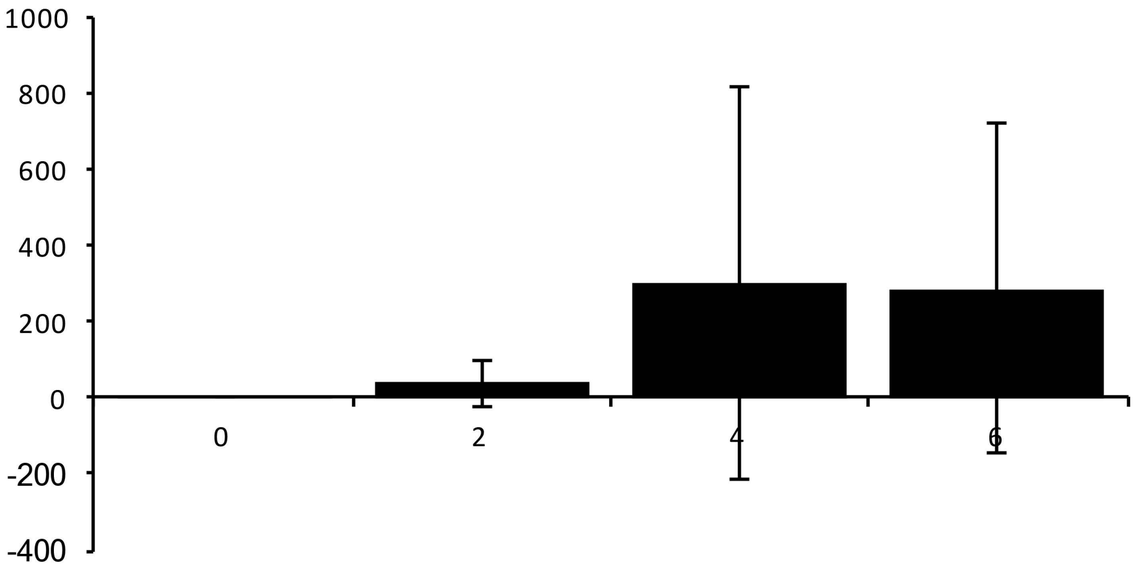

HME1 Anisomycin

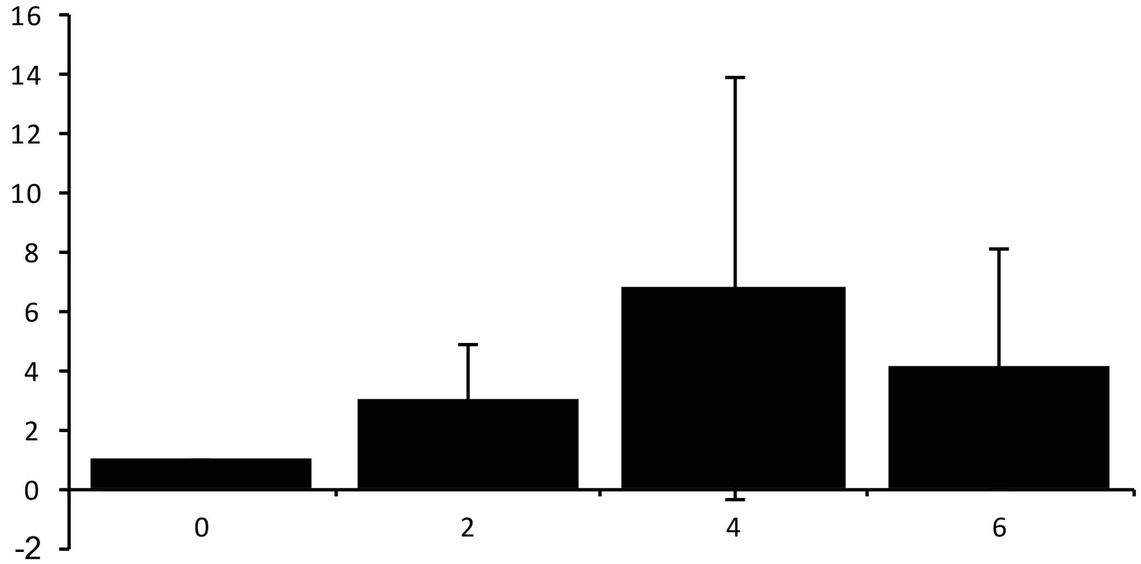

BJ Anisomycin

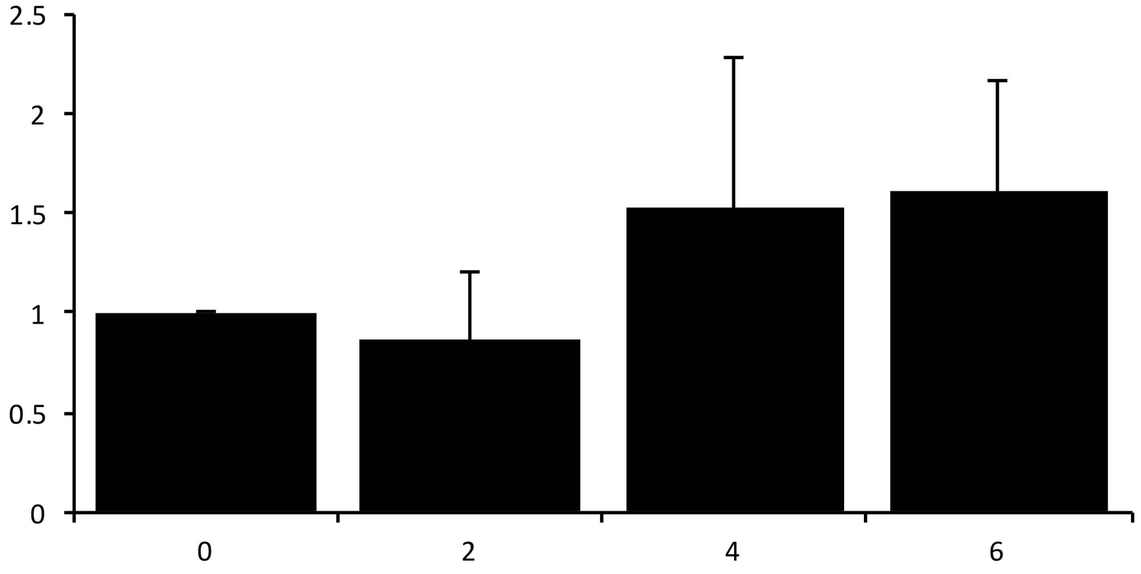

SF767 Anisomycin

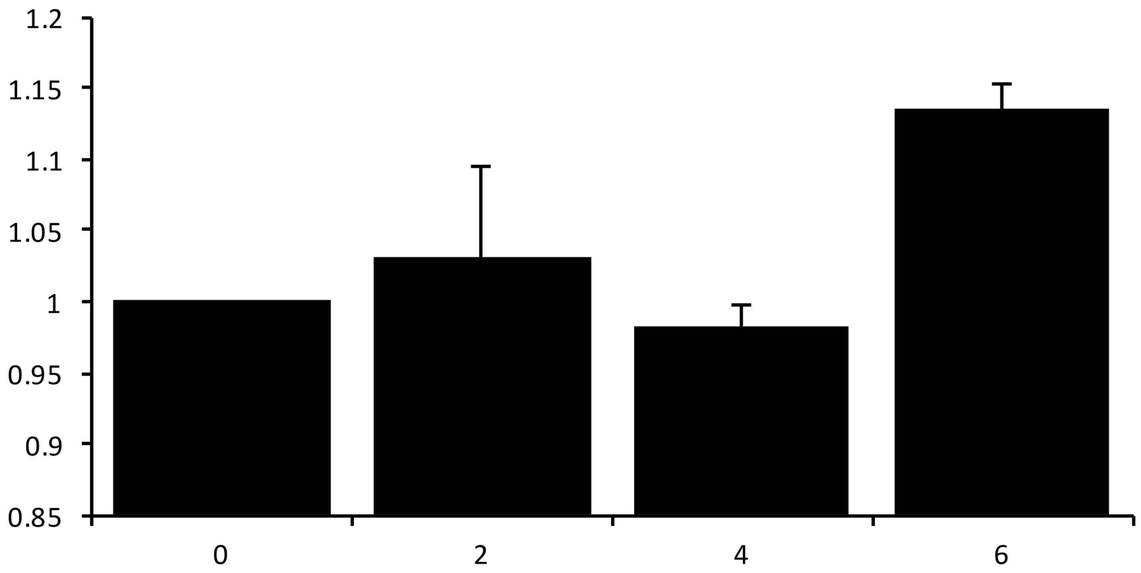

U87 Anisomycin

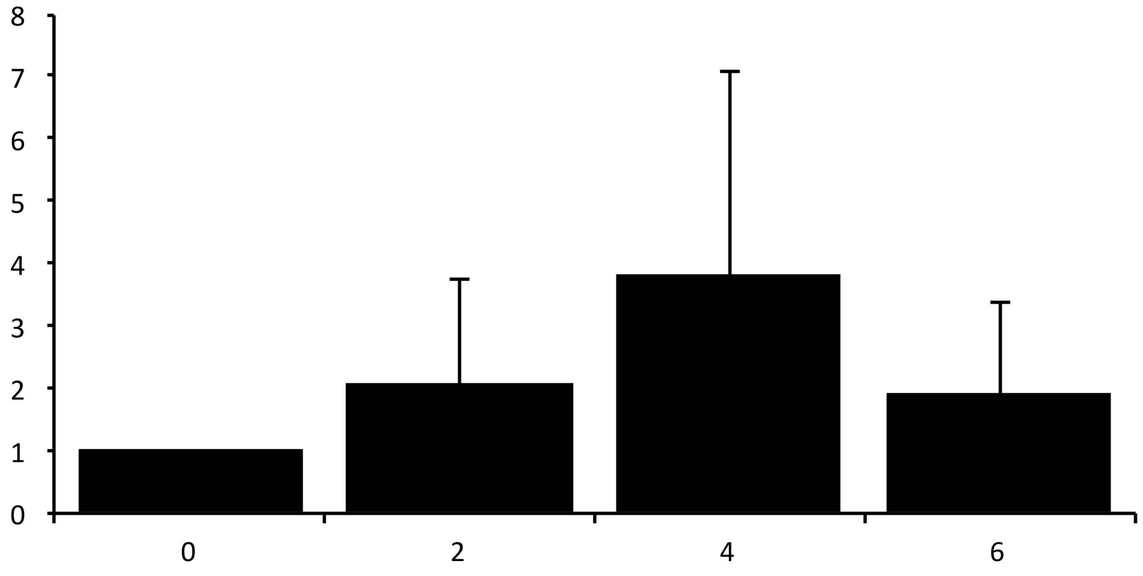

U87 Camptothecin